บรรณานุกรม

[1] วิบูลย์ แสงวีระพันธุ์ศิริ. รายงานการวิจัยเรื่อง Haptic System, โครงการวิจัยร่วมภาครัฐและเอกชนระบบผลิตอัตโนมัติเพื่อการพัฒนาอุตสาหกรรมการผลิตขั้นสูง กรกฎาคม 2548, หน้า 3-4.

[2] โอพาร วงศ์วิรัตน์. 2550. "การประยุกต์แฮปติกในทางการแพทย์." *[ระบบออนไลน์].* แหล่งที่มา http://blog.it.kmitl.ac.th/chotipat/archives/category/it-kmitl (22 มกราคม 2553)

[3] B. Hannaford and J. H. Ryu. (2002). "Time-Domain Passivity Control of Haptic Interfaces" *IEEE Trans. on Robotics and Automation*, 18 : 1-10.

[4] D. Oetomo, Q. H. Xia, M .H. Ang Jr., T.M. Lim, and S.Y. Lim. (2003). "Desing Issues and Requirements of a General Purpose Destop Haptic Interface" *PICS International conference and Exhibition on Instrumentation and Control*, 1-7.

[5] D. A. Lawrence. (1993). "Stability and Transparency in Bilateral Teleoperation" *IEEE Transactions on Robotics and Automation*, 9(5) : 624-637.

[6] D. Wang, K. Tuer, M. Rossi, L. Ni, and J. Shu. (2003). "The Effect of Time Delays on Tele-haptics" *Proc. IEEE Workshop on Haptic Audio Virtual Environments and Their Applications*, 7-12.

[7] G. Christiansson. (2004). "Measuring asymmetric haptic tele-operation device properties" *IEEE Conference on Systems Man and Cybernetics*, 3 : 2454-2458.

[8] G. R. Luecke. (1997). "Stability and Performance Comparison of the Force Reflecting Haptic Manipulator" *1997 8th International Conference on Advanced Robotics Proceedings ICAR97*, 673-642.

[9] J. H. Ryu, D. S. Kwon, and B. Hannaford. (2004). "Stable Teleoperation With Time-Domain Passivity Control" *IEEE Transactions on Robotics and Automation*,

20(2) : 365-373.

[10] J. Zhou, X. Shen, and N. D. Georganas. (2004). "Haptic Tela-Sugery Simulation" *Proceedings of the 3rd IEEE International Workshop on Haptic, Audio and Visual Environments and Their Applications,* 99-104.

[11] K. Hashtrudi-Zaad. (2001). "Analysis of Control Architectures for Teleoperation Systems with Inpedance/Admittance Master and Slave Manipulators" *The International Journal of Robotics Research*, 20(6) : 419-445.

[12] K. Hashtrudi-Zaad, and S. E. Salcudean. (2002) "Transparency in Time-Delayed Systems and the Effect of Local Force Feedback for Transparent Teleoperation" *IEEE Transactions on Robotics and Automation*, 18(1) : 108-114.

[13] K. park, W. K. Chung, and Y. Youm. (2004) "A New Position Error Based Robust Controller Design Framework of Teleoperation for Free to Contact Motion" *Proceeding of the 1992 IEEE International Conference on Robotics and Automation*, 4 : 4140-4146.

[14] M. Tavakoli, A Aziminejad, R.V. Patel, and M. Moallem. (2007). "Enhanced Transparency in Haptics-Based Master-Slave System" *Proceedings of the 2007 American Control Conference*, 1445-1460.

[15] M. Tavakoli, R. V. Patel, M. Moallem, and A. Aziminejad. (2008). "Haptics for Teleoperated Surgical Robotic Systems" *Europhysics Letters*, 1-179.

[16] M. Tavakoli, and R. D. Howe. (2009). "Haptic Effects of Sugical Teleoperator Flexibility" *The International Journal of Robotics Research*, 28(10) : 1289-1302.

[17] M. R. Sirouspour, S. P. DiMaio, S. E. Salcudean, P. Abolmaesumi, and C. Jones. (2000). "Haptic Interface Control Design Issues and Experiments with a Planar Device" *Proceeding of the 2000 IEEE International Conference on Robotics and Automation*, 1 : 789-794.

[18] P. Yen, R. D. Hibberd, and B. L. Davies. (1996). "A Telemanipulator System as an

Assistant and Training Tool for Penetrating Soft Tissue" *Mechatronics*, 6(4) : 423-436.

[19] R. J. Adams, and B. Hannaford. (1998). "A Two-Port Framework for the Design of the Unconditionally Stable Haptic Interfaces" *Proceeding of the 1998 IEEE/RSJ International Conference on Intelligent Robots and Systems*, 2 : 1254-1259.

[20] R.W. Daniel, and P. R. McAree. (1998). "Fundamental Limits of Performance for Force Reflecting Teleoperation" *The International Journal of Robotics Research*, 17(8) : 811-830.

[21] T. L. Brooks. (1990). "Telerobotic Response Requirements" *1990 IEEE International Conference on Systems Man and Cybernetics Conference Proceedings*, 113-120.

[22] T. Yoshikawa, and Y. Ichinoo. (2003). "Impedance Identification of Human Fingers Using Virtual Task Environment" *Proceeding of the 2003 IEEE/ASME International Conference on Advanced Intelligent Mechatronics*, 2 : 759-764.

[23] V. Hayward, and O. Astley. (1996). "Performance Measures for Haptic Interfaces" *1996 Robotics Research The 7th International Symposium*, 195-207.

[24] Y. Strassberg, A. A. Goldenberg, and J. K. Mills. (1992). "A New Control Scheme for Bilateral Teleoperating Systems: Performance Evaluation and Comparison" *Proceeding of the 1992 IEEE/RSJ International Conference on Intelligent Robots and Systems*, 2 : 865-872.

ภาคผนวก

ภาคผนวก ก

M-file และ Simulink

1. M-file สำหรับทำ FFT analysis ของสัญญาณแรงที่วัดได้จาก force sensor

```
%%%%%%%%%% FFT analysis for force signal %%%%%%%
clc;
clear;
load('fft_force_signal.mat')
t=fft_force_signal.X.Data ;
force_master=fft_force_signal.Y(1,1).Data ;
force_master_filter=fft_force_signal.Y(1,2).Data ;
force_slave=fft_force_signal.Y(1,3).Data  ;
force_slave_filter=fft_force_signal.Y(1,4).Data  ;

%%%%%%%%%%%%%%%%  master force (on power supply) %%%%%%%%%%%%%%%%%
figure(1)
subplot(2,1,1)
plot(t,force_master,'b') ;
xlabel('time(s)','fontsize',12)
ylabel('force(N)','fontsize',12)
title('force signal (on power supply)','fontsize',12)
axis([0 4 -2 2])
grid on
%%%%%%%%%%%%%%%%%% FFT & Amplitude analysis %%%%%%%%%%%%%%%%%
N=length(force_master);
Y=fft(force_master,N);
Py = Y.* conj(Y) / N;      %%%%%% The power spectrum
f = 33333*(0:N/2)/N;       %%%%%% Ts=0.00003 &  Graph the first haft of
N

subplot(2,1,2)
plot(f,Py(1:((N/2)+1)))
title('FFT-Analysis : frequency content of master force (on power
supply)','fontsize',12)
xlabel('frequency (Hz)')
ylabel('Amplitude')
axis([0 16000 0 800])
%%%%%%%%%%%%%%%%  master force (on power supply) %%%%%%%%%%%%%%%%%
figure(2)
plot(t,force_master,'r--') ;
hold on
plot(t,force_master_filter,'b') ;
hold off
xlabel('time(s)','fontsize',12)
ylabel('force(N)','fontsize',12)
%title('compare force with and without filter','fontsize',12)
legend('force signal','force singnal with low-pass filter',1)
axis([0 4 -2 2])
grid on
%%%%%%%%%%%%%%%%%%%%%%%%%%%%%%%%%%%%%%%%%%%%%%%%%%%%%%%%%%%%%%%%%%%%%%%
```

2. M-file : สำหรับออกแบบตัวควบคุม (design controller)

```
%%%%%%%%%%%%%%%%%%%%%%%% slave-controller %%%%%%%%%%%%%%%%%%%%%
clc;
clear;
s=tf('s');
G=1/((s^2)*4.4e-3);
imshow('xm2xs.jpg')

%%%%%%%%% P-controller(slave side)%%%
figure (1)
subplot(2,1,1)
rlocus(G)
subplot(2,1,2)
step( 1*G/(1+1*G) )
%%%%%%%%% PD-controller(slave side)%%%
k=15;
pd=(s+22);
figure (2)
subplot(2,1,1)
rlocus(pd*G)
subplot(2,1,2)
step( k*pd*G/(1+k*pd*G))
%%%%%%%%% PI-controller(slave side)%%%
kk=10;
PI=(s+1)/s;
figure (3)
subplot(2,1,1)
rlocus(PI*G)
subplot(2,1,2)
step( kk*PI*G/(1+kk*PI*G) )
%%%%%%%%% PID-controller (slave side)%%%
kkk=1;
PID=(s+5)*(s+20)/s;
figure (4)
subplot(2,1,1)
rlocus(PID*G)
subplot(2,1,2)
step( kkk*PID*G/(1+kkk*PID*G) )

%%%%%%%%%%%%% compare root rocus of ect system %%%%%%%%%%%
figure (5)
subplot(2,2,1)
rlocus(G)
title('root locus of the system (P-controller)','fontsize',10)
subplot(2,2,2)
rlocus(pd*G)
title('root locus of the system (PD-controller)','fontsize',10)
subplot(2,2,3)
rlocus(PI*G)
title('root locus of the system (PI-controller)','fontsize',10)
subplot(2,2,4)
rlocus(PID*G)
title('root locus of the system (PID-controller)','fontsize',10)
```

```
%%%%%%%%%%%%%%%%%%%%%%%% master-controller %%%%%%%%%%%%%%%%%
clc;
clear;
M=4.4e-3 ;  %%%% (Kg.m)
l=0.004 ;   %%%% (m)
s=tf('s');
Zh=(((3.06/1000)*s^2)+4.32*s+98.9) ; %%% human hand impedance
G=Zh/(M*s^2+(Zh*(l/2/pi)) )
figure(1)
rlocus(G)
axis([-110,0,-25,25])
ppp=pole(G)
ZZZ=zero(G)

%%%%%%%   P-controller  %%%%%%%%%%%%
Kp=0.12 ;
%%%%%%%%%%%%%%%% PD-controller %%%%%%%%%%%%%
K1=0.0006;
Kpd=tf([1 200],[0.0016 1]);  %%  with low-pass filter fc=100 Hz
Cpd=K1*Kpd;
%%%%%%%%%%%%%%% PI-controller %%%%%%%%%%%%%
K2=0.12;
Kpi=tf([1 10],[1 0.05]);     %%  with high-pass filter
Cpi=K2*Kpi;
%%%%%%%%%%%%%%% PID-controller %%%%%%%%%%%%%
K3=0.4;
Kpid=(s+200)*(s+10)/((s+0.05)*(s+625));     %%%% with filter
Cpid=K3*Kpid;
%%%%%%%%%%  step response %%%%%%%%%%%%%%%%%%
sys_close=(Zh*Cpd)/((M*s^2)+(Zh*(l/2/pi))+(Zh*Cpd)) ; %%%% system
close loop for PD-controller
figure(2)
step(sys_close)
axis([0 0.3 0 1.2])
xlabel('time','fontsize',12)
ylabel('force(N)','fontsize',12)
grid on
%%%%%%%%%%%%%%%%%% root locus %%%%%%%%%%%%%%%
figure(3)
subplot(2,2,1)
rlocus(G)
title('root locus of the master system (P-controller)','fontsize',12)
axis([-160 5 -25 25])
subplot(2,2,2)
rlocus(Kpd*G)
title('root locus of the master system (PD-
controller)','fontsize',12)
axis([-210 5 -25 25])
subplot(2,2,3)
rlocus(Kpi*G)
title('root locus of the master system (PI-
controller)','fontsize',12)
axis([-160 5 -35 35])
subplot(2,2,4)
rlocus(Kpid*G)
title('root locus of the master system (PID-
controller)','fontsize',12)
axis([-210 5 -30 30])
```

```
figure(4) %%%% frequency response for PD-controller %%%%
bode((Zh*Cpd)/((M*s^2)+(Zh*(1/2/pi))+(Zh*Cpd)),'k',{10^-1, 2000})
grid on
```

3. Simulink สำหรับการควบคุมตำแหน่งการเคลื่อนที่ด้านสเลฟ

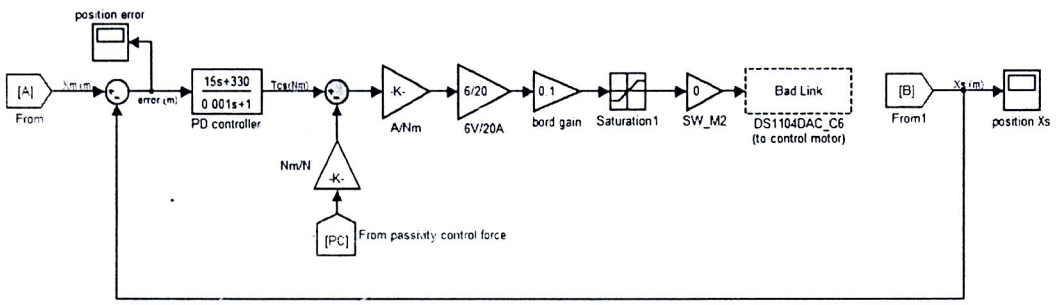

รูป ก1 Simulink สำหรับการควบคุมตำแหน่งการเคลื่อนที่ด้านสเลฟ

4. Simulink สำหรับการควบคุมแรงทางด้านมาสเตอร์

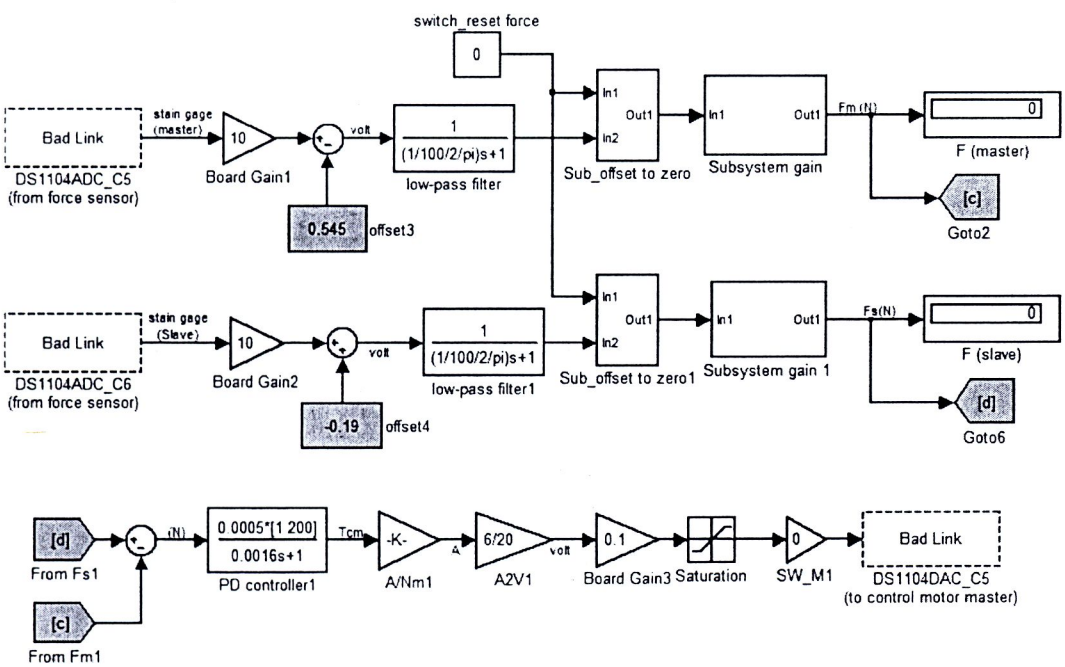

รูป ก2 Simulink สำหรับการควบคุมแรงทางด้านมาสเตอร์

5. Simulink สำหรับการควบคุม Passivity

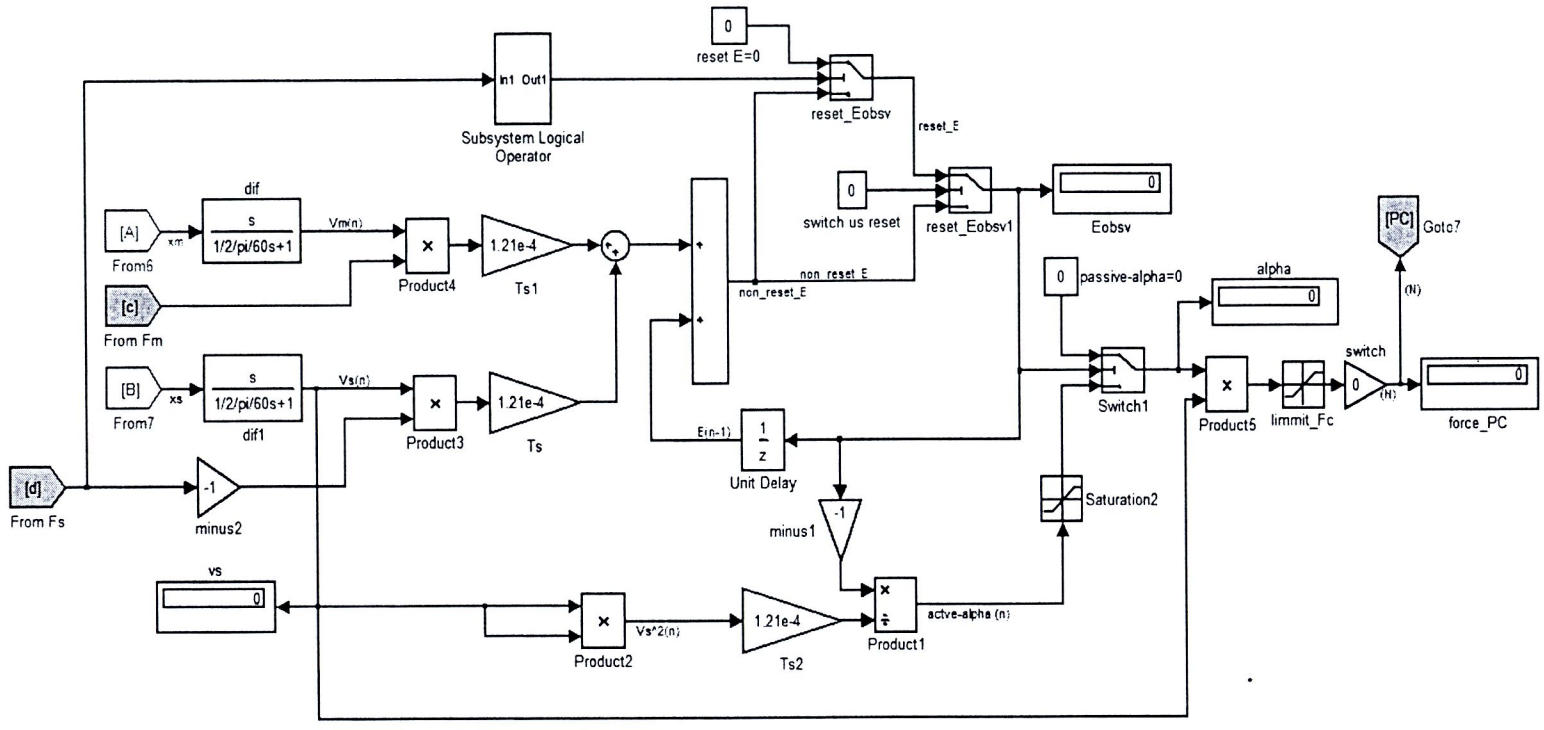

รูป ก3 Simulink สำหรับการควบคุม Passivity

ภาคผนวก ข

อุปกรณ์ที่ใช้ในการสร้างระบบแฮปติก

1. อุปกรณ์ขยายสัญญาณ

BURR-BROWN®

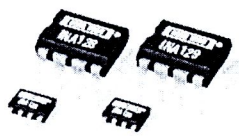

INA128
INA129

Precision, Low Power INSTRUMENTATION AMPLIFIERS

FEATURES

- LOW OFFSET VOLTAGE: 50μV max
- LOW DRIFT: 0.5μV/°C max
- LOW INPUT BIAS CURRENT: 5nA max
- HIGH CMR: 120dB min
- INPUTS PROTECTED TO ±40V
- WIDE SUPPLY RANGE: ±2.25 to ±18V
- LOW QUIESCENT CURRENT: 700μA
- 8-PIN PLASTIC DIP, SO-8

APPLICATIONS

- BRIDGE AMPLIFIER
- THERMOCOUPLE AMPLIFIER
- RTD SENSOR AMPLIFIER
- MEDICAL INSTRUMENTATION
- DATA ACQUISITION

DESCRIPTION

The INA128 and INA129 are low power, general purpose instrumentation amplifiers offering excellent accuracy. Their versatile 3-op amp design and small size make them ideal for a wide range of applications. Current-feedback input circuitry provides wide bandwidth even at high gain (200kHz at G = 100).

A single external resistor sets any gain from 1 to 10,000. INA128 provides an industry standard gain equation; INA129's gain equation is compatible with the AD620.

The INA128/INA129 is laser trimmed for very low offset voltage (50μV), drift (0.5μV/°C) and high common-mode rejection (120dB at G ≥ 100). It operates with power supplies as low as ±2.25V, and quiescent current is only 700μA—ideal for battery operated systems. Internal input protection can withstand up to ±40V without damage.

The INA128/INA129 is available in 8-pin plastic DIP, and SO-8 surface-mount packages, specified for the –40°C to +85°C temperature range. The INA128 is also available in dual configuration, the INA2128.

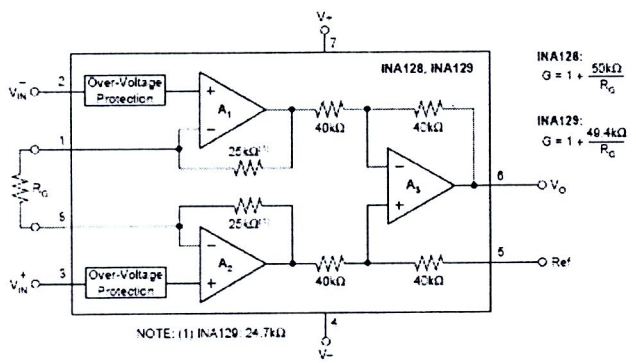

International Airport Industrial Park • Mailing Address: PO Box 11400, Tucson, AZ 85734 • Street Address: 6730 S. Tucson Blvd., Tucson, AZ 85706 • Tel: (520) 746-1111 • Twx: 910-952-1111
Internet: http://www.burr-brown.com/ • FAXLine: (800) 548-6133 (US/Canada Only) • Cable: BBRCORP • Telex: 066-6491 • FAX: (520) 889-1510 • Immediate Product Info: (800) 548-6132

PDS-1296C

Printed in U.S.A. October, 1996

APPLICATION INFORMATION

Figure 1 shows the basic connections required for operation of the INA128/INA129. Applications with noisy or high impedance power supplies may require decoupling capacitors close to the device pins as shown.

The output is referred to the output reference (Ref) terminal which is normally grounded. This must be a low-impedance connection to assure good common-mode rejection. A resistance of 8Ω in series with the Ref pin will cause a typical device to degrade to approximately 80dB CMR (G = 1).

SETTING THE GAIN

Gain is set by connecting a single external resistor, R_G, connected between pins 1 and 8:

INA128:
$$G = 1 + \frac{50k\Omega}{R_G} \quad (1)$$

INA129:
$$G = 1 + \frac{49.4k\Omega}{R_G} \quad (2)$$

Commonly used gains and resistor values are shown in Figure 1.

The 50kΩ term in Equation 1 (49.4kΩ in Equation 2) comes from the sum of the two internal feedback resistors of A_1 and A_2. These on-chip metal film resistors are laser trimmed to accurate absolute values. The accuracy and temperature coefficient of these internal resistors are included in the gain accuracy and drift specifications of the INA128/INA129.

The stability and temperature drift of the external gain setting resistor, R_G, also affects gain. R_G's contribution to gain accuracy and drift can be directly inferred from the gain equation (1). Low resistor values required for high gain can make wiring resistance important. Sockets add to the wiring resistance which will contribute additional gain error (possibly an unstable gain error) in gains of approximately 100 or greater.

DYNAMIC PERFORMANCE

The typical performance curve "Gain vs Frequency" shows that, despite its low quiescent current, the INA128/INA129 achieves wide bandwidth, even at high gain. This is due to the current-feedback topology of the input stage circuitry. Settling time also remains excellent at high gain.

NOISE PERFORMANCE

The INA128/INA129 provides very low noise in most applications. Low frequency noise is approximately 0.2μVp-p measured from 0.1 to 10Hz (G ≥ 100). This provides dramatically improved noise when compared to state-of-the-art chopper-stabilized amplifiers.

INA128: $G = 1 + \frac{50k\Omega}{R_G}$ INA129: $G = 1 + \frac{49.4k\Omega}{R_G}$

DESIRED GAIN (V/V)	INA128 R_G (Ω)	INA128 NEAREST 1% R_G (Ω)	INA129 R_G (Ω)	INA129 NEAREST 1% R_G (Ω)
*	NC	NC	NC	NC
2	50.00k	49.9k	49.4k	49.9k
5	12.50k	12.4k	12.35k	12.4k
10	5.556k	5.62k	5489	5.49k
20	2.632k	2.61k	2600	2.61k
50	1.02k	1.02k	1005	1k
100	505.1	511	499	499
200	251.3	249	248	249
500	100.2	100	99	100
1000	50.05	49.9	49.5	49.9
2000	25.01	24.9	24.7	24.9
5000	10.00	10	9.88	9.76
10000	5.001	4.99	4.94	4.87

NC: No Connection.

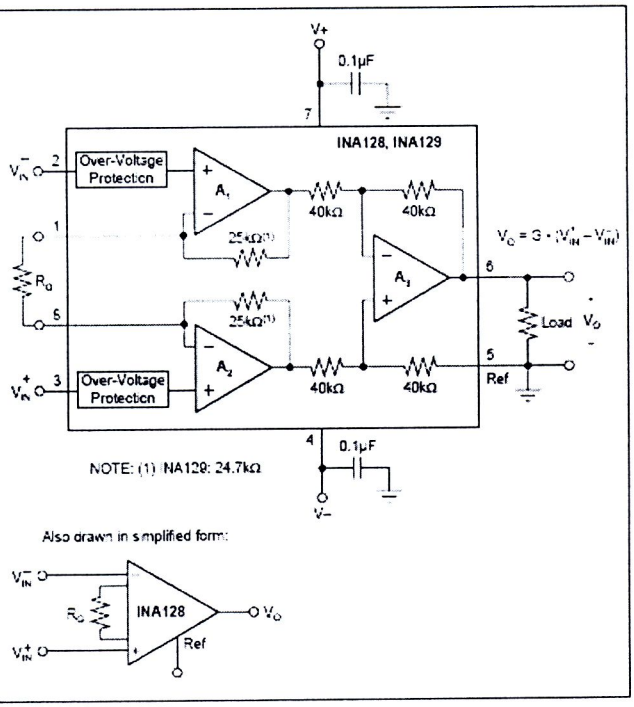

FIGURE 1. Basic Connections.

OFFSET TRIMMING

The INA128/INA129 is laser trimmed for low offset voltage and offset voltage drift. Most applications require no external offset adjustment. Figure 2 shows an optional circuit for trimming the output offset voltage. The voltage applied to Ref terminal is summed with the output. The op amp buffer provides low impedance at the Ref terminal to preserve good common-mode rejection.

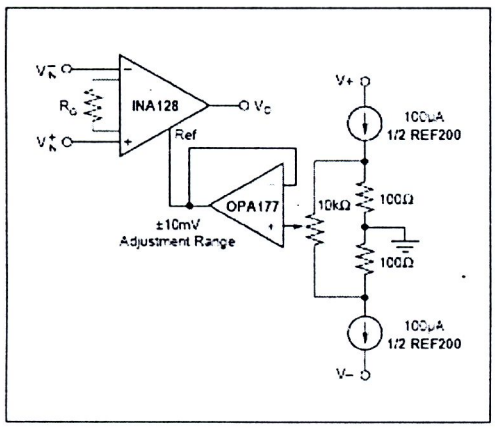

FIGURE 2. Optional Trimming of Output Offset Voltage.

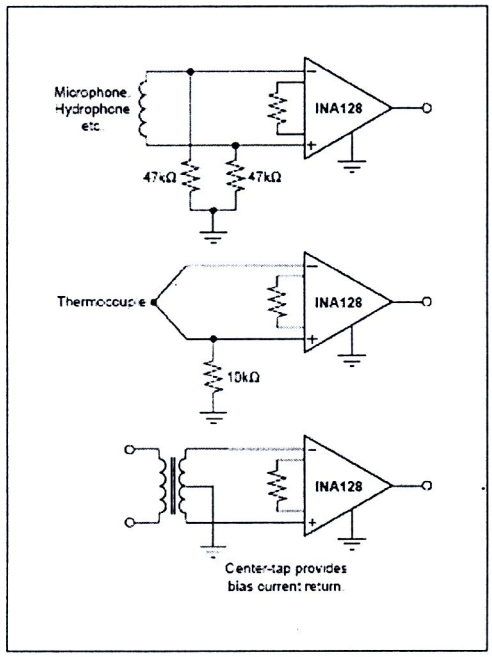

FIGURE 3. Providing an Input Common-Mode Current Path.

INPUT BIAS CURRENT RETURN PATH

The input impedance of the INA128/INA129 is extremely high—approximately $10^{10}\Omega$. However, a path must be provided for the input bias current of both inputs. This input bias current is approximately ±2nA. High input impedance means that this input bias current changes very little with varying input voltage.

Input circuitry must provide a path for this input bias current for proper operation. Figure 3 shows various provisions for an input bias current path. Without a bias current path, the inputs will float to a potential which exceeds the common-mode range, and the input amplifiers will saturate.

If the differential source resistance is low, the bias current return path can be connected to one input (see the thermocouple example in Figure 3). With higher source impedance, using two equal resistors provides a balanced input with possible advantages of lower input offset voltage due to bias current and better high-frequency common-mode rejection.

INPUT COMMON-MODE RANGE

The linear input voltage range of the input circuitry of the INA128/INA129 is from approximately 1.4V below the positive supply voltage to 1.7V above the negative supply. As a differential input voltage causes the output voltage increase, however, the linear input range will be limited by the output voltage swing of amplifiers A_1 and A_2. So the linear common-mode input range is related to the output voltage of the complete amplifier. This behavior also depends on supply voltage—see performance curves "Input Common-Mode Range vs Output Voltage".

Input-overload can produce an output voltage that appears normal. For example, if an input overload condition drives both input amplifiers to their positive output swing limit, the difference voltage measured by the output amplifier will be near zero. The output of A_3 will be near 0V even though both inputs are overloaded.

LOW VOLTAGE OPERATION

The INA128/INA129 can be operated on power supplies as low as ±2.25V. Performance remains excellent with power supplies ranging from ±2.25V to ±18V. Most parameters vary only slightly throughout this supply voltage range—see typical performance curves. Operation at very low supply voltage requires careful attention to assure that the input voltages remain within their linear range. Voltage swing requirements of internal nodes limit the input common-mode range with low power supply voltage. Typical performance curves, "Input Common-Mode Range vs Output Voltage" show the range of linear operation for ±15V, ±5V, and ±2.5V supplies.

2. อุปกรณ์ขับกระแส

MODELS 4122Z, 4212Z
DC BRUSH SERVO AMPLIFIERS

FEATURES

- *No zero-current deadband*
- *Only one potentiometer!*
- Component socket configures amp completely
- *Flexibility!* Internal 40-pin socket configures amp with no soldering
- Separate current limits: Continuous, peak, and peak-time
- No integrator windup when disabled
- Fault protections:
  Short-circuits from output to output, output to gnd
  Over/under voltage
  Over temperature
  Self-reset or latch-off modes
- 3kHz Bandwidth
- Wide load inductance range: 0.4-40 mH.
- Surface mount technology construction, lower part count.

APPLICATIONS

- Voice coil motors
- X-Y stages
- Automated assembly machinery
- Magnetic bearings

THE OEM ADVANTAGE

- Same package as 4122, 4212 models lets system designers 'mix and match' types.
- Conservative design for high MTBF
- No soldering required to change header parts.
- Custom configurations available (contact factory)
  No-pots, custom headers

MODEL	POWER	I-CONT	I-PEAK
4122Z	+22 to +90 VDC	10	20
4212Z	+22 to +125 VDC	6	12

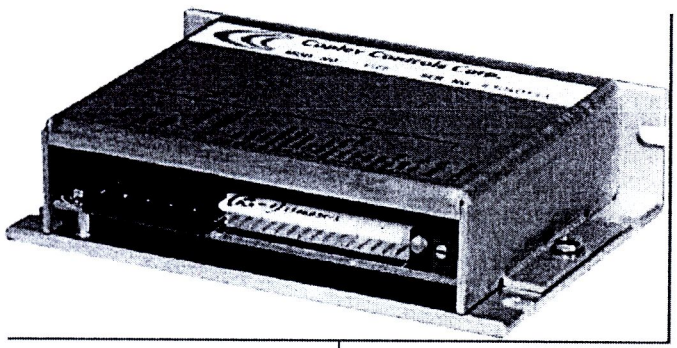

FEATURES

"Z" versions of 4122 and 4212 models feature 50% modulation that delivers no zero-current deadband for applications that require fine motion around zero such as voice coil motors, laser focusing, and wire bonding.

Models are mechanically identical to 4122 and 4212 types so that system builders can 'mix and match' with a common mounting scheme.

Built using surface-mount technology, these amplifiers offer plug and play operation in a very small package. All models take industry standard ±10V control signals as input, and operate motors in torque mode, or velocity mode using analog brush tachometers.

Velocity loops using brush-tachometer feedback are used for open-loop speed controls, or in position control loops requiring improved regulation at low speeds.

Model 4122Z operates from −22 to −90VDC unregulated power supplies, and outputs 10A continuous, 20A peak.

Model 4212Z operates from −22 to −125VDC power supplies, and outputs 6A continuous, and 12A peak.

The active logic-level of the amplifier Enable input is jumper selectable to GND or +5V to interface with different control cards. /Pos and /Neg enable inputs remain ground active for fail-safe operation.

Mosfet H-bridge output stage delivers power in four-quadrants for bi-directional acceleration and deceleration of motors.

An internal solderless socket holds 17 components that configure the various gain and current limit settings to customize the amplifiers for a wide range of loads and applications.

Header components permit compensation over a wide range of load inductances to maximize bandwidth with different motors.

Individual peak and continuous current limits allow high acceleration without sacrificing protection against continuous overloads. Peak current time limit is settable to match amplifier to motor thermal or commutation limits.

All models are protected against output short circuits (output to output and output to ground) and heatplate overtemperature.

With the /Reset input open, output shorts or heatplate overtemperature will latch off the amplifier until power is cycled off & on, or until the /Reset input is grounded. For self-reset from such conditions, wire /Reset to ground and the amplifier will reset every 200ms.

A bicolor led speeds diagnostics during set-up, or for fault isolation after the unit is in service.

Copley Controls, 20 Dan Road, Canton, MA 02021 Tel: 781-828-8090 Fax:781-828-6547

3. อุปกรณ์วัดตำแหน่ง (incremental encoder)

US DIGITAL **E4P** OEM Miniature Optical Kit Encoder
Page 1 of 8

RoHS COMPLIANT

Description

The E4P miniature encoder is designed to provide digital quadrature encoder feedback for high volume applications with limited space constraints. The E4P version utilizes an innovative, patented push-on codewheel which accepts shaft diameters of 1.5mm to .250".

The E4P encoder is the leader for high quantity OEM applications, but the E4 is the ideal choice when a set-screw codewheel encoder is required (see the E4 page).

The E4P miniature encoder base provides mounting holes for two #3-48, length 1/4" or two M2.5x.45mm, length 6mm screws on a .555" bolt circle. When mounting holes are not available, a pre-applied transfer adhesive (with peel-off backing) is available for "stick-on" mounting.

The encoder cover is easily snapped onto the base and is embossed with the connector pin-out.

The E4P series encoder can be connected by using a (high retention 4-conductor snap-in polarized 1.25mm pitch) connector. Mating cables and connectors (see the Cables / Connectors web page) are not included and are available separately.

Features

- Miniature size
- Push-on hub - spring loaded collet design
- Minimum shaft length of .375"
- Fits shaft diameters of .059" to .250"
- Accepts +/-.020" Axial shaft play
- Off-axis mounting tolerance of .010"
- 100 to 360 cycles per revolution (CPR)
- 400 to 1440 pulses per revolution (PPR)
- Single +5V supply

Related Products & Accessories

- CA-FC5-SH-MIC4 5-Pin Latching / 4-Pin Micro Shielded Cable (Base price $15.15)
- CA-MD6-SS-MIC4 6-Pin Modular / 4-Pin Micro Silver Satin Cable (Base price $11.53)
- CA-MIC4-S--NC 4-Pin Micro / Unterminated Shielded Cable (Base price $7.30)
- CA-MIC4-W4-NC 4-Pin Micro / Unterminated 4-Wire Discrete Cable (Base price $6.80)
- CON-MIC4 4-Pin Micro Connector (Base price $3.15)
- MCTOOL Centering Tool for E4, E4P, and E5P (Base price $5.25)
- SPACER Spacer Tool (Base price $0.95)

Mechanical Drawing

US DIGITAL
1400 NE 136th Avenue
Vancouver, Washington 98684, USA
info@usdigital.com
www.usdigital.com
Local: 360.260.2468
Toll-free: 800.736.0194

4. มอเตอร์กระแสตรง

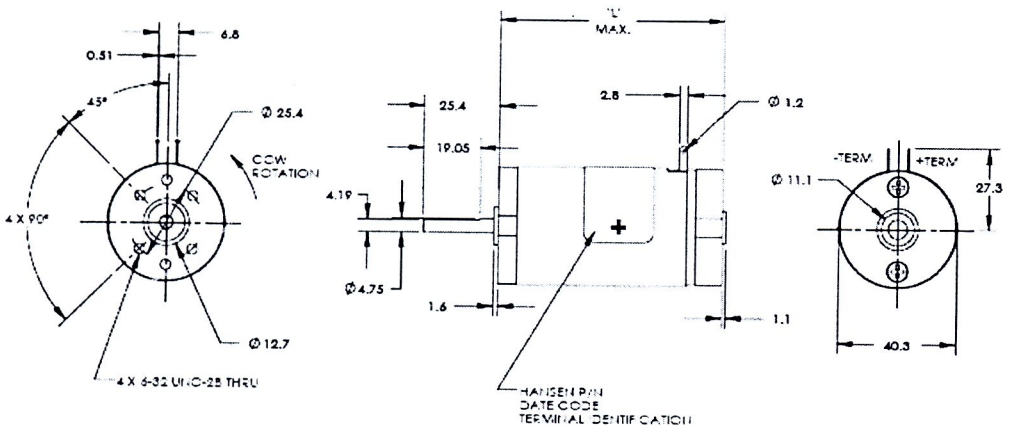

ตาราง ข1 ข้อมูลทั่วไปของมอเตอร์กระแสตรง

Matric Specifications Switch to English

Part Number	Rated Voltag	No Load		Rated Load					Stall		Voltage Constant	Torque Constant	Terminal Resistanc	"L" Dimensio
	Volts	Speed RPM	Current Amps	Torque mNm	Speed RPM	Current Amps	Power Watts	Efficie %	Torque mNm	Current Amps	V/kRPM	mNm/A	Ohms	mm
116-1271216	12	2750	0.1	49	1700	1.3	9	55%	130	3.2	5.2	49	4.64	68.3
116-1321216	12	2400	0.1	71	1700	1.7	13	62%	238	5.3	4.8	46	2.22	80.3
116-1271232	12	4100	0.2	42	3300	1.7	15	71%	212	7.6	2.8	27	1.26	68.3
116-1321232	12	4000	0.2	64	3300	2.6	22	71%	347	12.8	2.9	28	0.84	80.3
116-1271248	12	5800	0.3	42	4850	2.5	22	71%	272	14.4	2	19	0.7	68.3
116-1321248	12	5450	0.4	64	4750	3.6	32	74%	496	25.2	2.1	20	0.38	80.3
116-1272416	24	2750	0.1	49	1700	0.7	9	53%	130	1.6	8.5	81	14.97	68.3
116-1322416	24	2450	0.1	71	1700	0.8	13	62%	232	2.5	9.6	92	8.9	80.3
116-1272432	**24**	**4150**	**0.1**	**42**	**3300**	**1**	**15**	**64%**	**212**	**4.1**	**5.7**	**54**	**5.61**	**68.3**
116-1322432	24	4100	0.1	64	3350	1.3	22	71%	350	6.4	5.8	55	3.32	80.3
116-1272448	24	5750	0.2	42	4900	1.2	22	73%	286	7.5	4	39	2.83	68.3
116-1322448	24	5500	0.2	64	4800	1.7	32	77%	551	14.6	4.3	42	1.57	80.3

ที่มา : http://www.hansen-motor.com/brush-16.php

ประวัติผู้เขียน

ชื่อ-สกุล	นายณัฐชัย โปธิ
วัน เดือน ปี เกิด	22 มกราคม 2527
ประวัติการศึกษา	สำเร็จการศึกษามัธยมศึกษาตอนปลาย โรงเรียนสันป่าตองวิทยาคม จ. เชียงใหม่ ปีการศึกษา 2544 สำเร็จการศึกษาปริญญาวิศวกรรมศาสตรบัณฑิต สาขาวิชาวิศวกรรมเครื่องกล มหาวิทยาลัยเทคโนโลยีสุรนารี จ. นครราชสีมา ปีการศึกษา 2549
ประสบการณ์	วิศวกรออกแบบแม่พิมพ์ บริษัท ไทยสแตนเลย์การไฟฟ้า จำกัด (มหาชน) ในปี 2549-2551
ผลงานวิจัย	ตีพิมพ์บทความเรื่อง “การออกแบบและควบคุมระบบแฮปติกอินเตอร์เฟส 1 องศาอิสระ” การประชุมวิชาการวิศวกรรมวิจัยเพื่อพัฒนาประเทศไทย ครั้งที่ 1 (NCERTD-1) หน้า 37-38